ChemPubSoc Europe

DOI: 10.1002/open.201500201

Open Access ChemistryOPEN Full Papers

Effect of Amide Hydrogen Bonding Interaction on Supramolecular Self-Assembly of Naphthalene Diimide Amphiphiles with Aggregation Induced Emission

Namdev V. Ghule,[a] Duong Duc La,[b] Rajesh S. Bhosale,[a] Mohammad Al Kobaisi,[b] Aaron M. Raynor,[b] Sheshanath V. Bhosale,*[b] and Sidhanath V. Bhosale*[a]

In the present work, two new naphthalene diimide (NDI) amphiphiles, **NDI-N** and **NDI-NA**, were successfully synthesized and employed to investigate their self-assembly and optical properties. For **NDI-NA**, which contains an amide group, aggregation-induced emission enhancement (AIEE) was demonstrated in the presence of various ratios of methylcyclohexane (MCH) in chloroform, which led to the visual color changes. This new amide-containing **NDI-NA** amphiphile formed nanobelt structures in chloroform/MCH (10:90, *v/v*) and microcup-like morphologies in chloroform/MCH (5:95, *v/v*). The closure of these microcups led to the formation of vesicles and microcapsules. The structural morphologies gained from the solvophobic control of **NDI-NA** were confirmed by various complementary techniques such as infrared spectroscopy, X-ray diffraction, and scanning and transmission electron microscopy. In the absence of the amide moiety in **NDI-N**, no self-assembly was observed, indicating the fundamental role of H-bonding in the self-association process.

Introduction

Supramolecular self-assembly and the self-organization of molecules play an important role in the construction of thermodynamically stable structures at both the cellular and subcellular level, within nanometer to millimeter dimensions, and utilizes a 'bottom-up' or 'bio-inspired' approach.[1] Interest in supramolecular self-assembly using various functional π-systems has grown significantly in recent years.[2] Such supramolecular materials with defined photophysical properties are potential candidates for applications in areas ranging from organic electronics to the biological sciences.[3] The intermolecular amide–amide hydrogen bonding in supramolecular chemistry promotes the fabrication of well-defined assemblies and has recently led to new functional electronic materials.[4] Naphthalene diimide (NDI) chromophores[5] have drawn considerable attention due to their unique optical and electronic properties, which have led to various applications in sensors,[4] semiconductor devices,[2b,6] organic phtovoltaic devices,[7] and artificial photosynthesis,[8] as well as biological applications.[9] Furthermore, NDI derivatives have been extensively investigated in the field of supramolecular self-assembly to produce well-defined nanostructures such as nanobelts,[10] nanotubes,[2f,11] ion channels,[12] hydrogels,[13] organogels,[14] catenanes,[15] rotaxanes,[16] foldamers,[17] nanoparticles,[18] stimuli responsive nanomaterials,[19] and aggregation-induced emission enhancement (AIEE)[20] nanostructures.

In recent years, AIEE-activity has emerged as an important property of self-aggregating materials, and has attracted much attention. Due to their excellent spectroscopic properties such as large molar extinction coefficients (Φ) and high fluorescence quantum yields, these materials have seen applications in areas such as biology.[21] The typical restricted intramolecular rotation: a mechanism for aggregation-induced emission has been proposed by Tang et al.,[22] and other mechanisms such as the *J* aggregation,[23] hydrophilic interaction,[24] and excimer formation[25] have been reported in the literature. Although considerable progress has been made over the last several years,[26] there is still a need to design and engineer new AIEE[27] systems to produce new functional luminescent materials for specific applications.

In this work, we report the synthesis, self-assembly, and AIEE properties of **NDI-N** and **NDI-NA** derivatives. Characteristically, the **NDI-NA** molecule possess three important properties resulting in the formation of various nanostructures through solvent control: 1) the aromatic core of the NDI, which is designed to optimize the dispersive interactions (π–π-stacking) between the cores within a construct, 2) amide linkage that tackles the strong hydrogen bonding within the assembly, and 3) hydrophobic alkyl chains that help maximize the influence

[a] *N. V. Ghule, Dr. R. S. Bhosale, Dr. S. V. Bhosale*
Polymers and Functional Materials Division
CSIR-Indian Institute of Chemical Technology
Hyderabad, Telangana 500 007 (India)
E-mail: bhosale@iict.res.in
bhosale.iict@gov.in

[b] *D. D. La, Dr. M. Al Kobaisi, A. M. Raynor, Dr. S. V. Bhosale*
School of Applied Sciences, RMIT University
GPO Box 2476, Melbourne, VIC 3001 (Australia)
E-mail: sheshanath.bhosale@rmit.edu.au

Supporting information for this article is available on the WWW under http://dx.doi.org/10.1002/cplu.201500201.

of solvents. These arrangements prevent crystallization and favor the directional growth of the nanostructure in a one- to three-dimensional fashion (Figure 1).

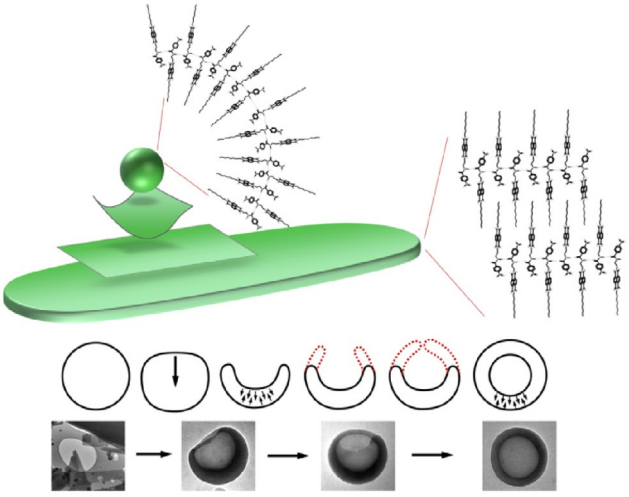

Figure 1. NDI-NA molecules self-assembled into supramolecular microsheets via amide H-bonding, π–π stacking, and hydrophobic interaction. The microsheet bilayer detaches from other microsheets layer-by-layer upon solvent evaporation. Furthermore, the nanosheets are transformed into microcups, which turn into microcapsules (vesicles).

Interestingly, **NDI-NA** exhibits very unique AIEE phenomenon with a significantly enhanced emission intensity in aggregation state. However, compound **NDI-N** without amide linkage failed to produce any defined nanostructures.

Results and Discussion

The synthetic strategy of the **NDI-N** and **NDI-NA** is shown in Scheme 1. The monoimidation was carried out using naphthalene dianhydride **1** with octylamine in a mixture of *n*-propanol and water at 50 °C under nitrogen atmosphere, yielding **2** in 74%. The **NDI-N** was synthesized by setting a mixture of **2** and *p*-amino nitrobenzene in dimethyl formamide (DMF) for at reflux 12 h, yielding **NDI-N** in 70% (Scheme 1). The synthesis of compound **NDI-NA** started from **2**, which was converted to **3** using mono-boc-ethylenediamine in triethylamine at reflux (90 °C). Compound **4** was obtained through a reaction between NDI **3** and trifluoroacetic acid (TFA) in dichloromethane. NDI **4** with 4-nitrobenzoic acid in the presence of triethylamine led to formation of **NDI-NA** in 62% yield.

The UV/Vis absorption and fluorescence emission spectra of **NDI-N** amphiphile in chloroform at room temperature are shown in Figure 2 A and B, respectively. The UV/Vis absorption spectrum of **NDI-N** amphiphile in chloroform exhibits two peaks with a maximum at 380 nm and a second absorption band appearing at 358 nm, along with a shoulder peak at 340 nm, which is attributed to the π–π* transitions of naphthalene diimide core.[28] Figure 2 A shows the UV/Vis absorption spectroscopic changes of **NDI-N** in chloroform with the gradual addition of methylcyclohexane (MCH, 0–95%) at room temperature. When MCH (0–95%) was added into the chloroform solution of **NDI-N**, the intensity of the absorption maximum at 358 and 380 nm (π–π* transitions of NDI core) gradually decreased with a coinciding blue shift. But the decrease in intensity was insignificant. The fluorometric response of **NDI-N** was

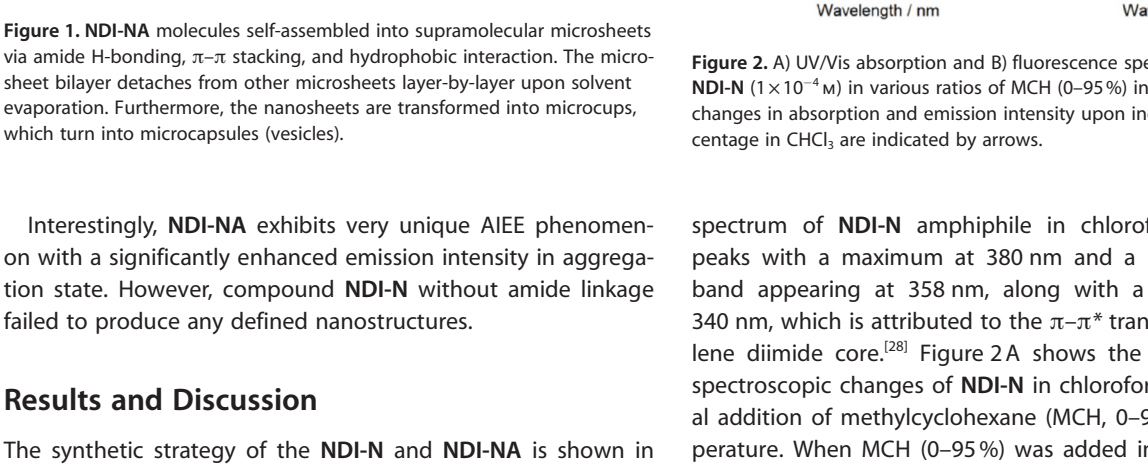

Figure 2. A) UV/Vis absorption and B) fluorescence spectra ($\lambda_{ex} = 350$ nm) of **NDI-N** (1×10^{-4} M) in various ratios of MCH (0–95%) in $CHCl_3$ at rt. The changes in absorption and emission intensity upon increasing the MCH percentage in $CHCl_3$ are indicated by arrows.

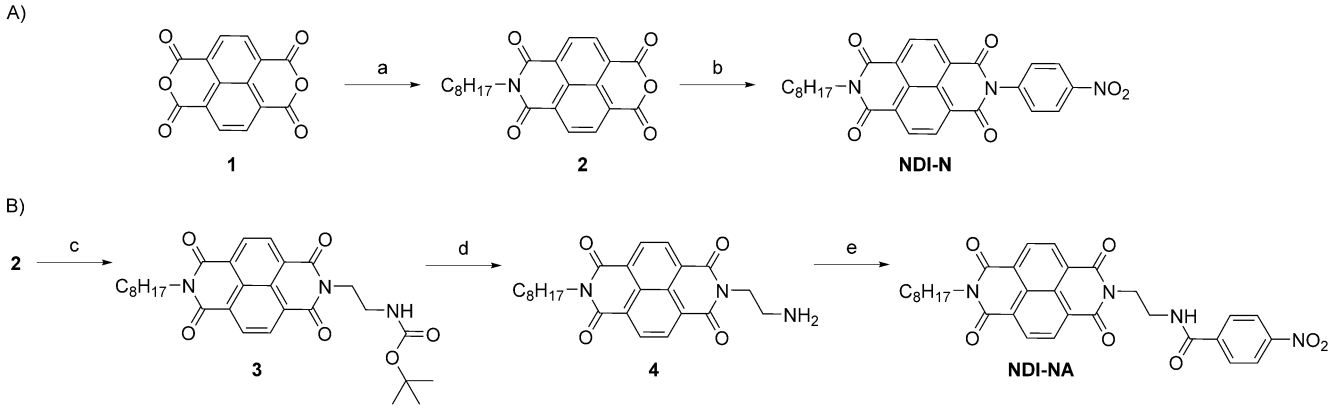

Scheme 1. Synthesis of NDI amphiphiles. *Reagents and conditions*: A) a) *n*-propanol + H_2O (1:1), octyl amine, 50 °C, 24 h, N_2 atm., 74%; b) 4-nitroaniline, DMF, reflux, 12 h, N_2 atm., 70%; B) c) mono-boc-ethylenediamine, Et_3N, *i*PrOH, 72 h, 90 °C, 78%; d) TFA:CH_2Cl_2 (1:1), 3 h, 96%; e) $SOCl_2$, DMF, 4-nitrobenzoic acid, CH_2Cl_2, Et_3N, 12 h, rt, 62%.

also investigated in chloroform. Upon excitation ($\lambda_{ex}=350$ nm), **NDI-N** exhibited two fluorescence bands with a maximum at 421 nm, 446 nm, and 472 nm, which could be attributed to the characteristic emission of NDI core. The titration experiment was conducted with the MCH (0–95%) addition to the chloroform solution of **NDI-N**, no significant enhancement of emission intensity was observed, that is, fluorescence quantum efficiency ($\Phi_F=2.4\%$) as depicted in Figure 2B. This indicated that **NDI-N** does not show an AIEE effect.

Figure 3A shows that the UV/Vis absorption spectra of **NDI-NA** in chloroform exhibits typical three absorption bands at

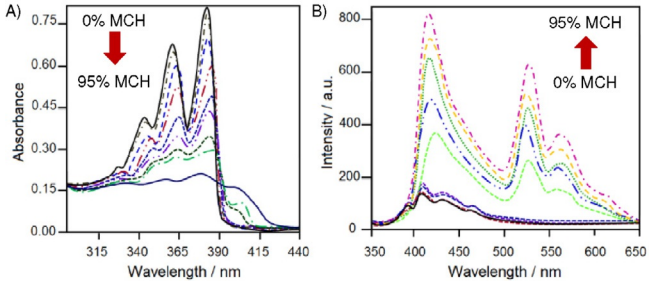

Figure 3. A) UV/Vis absorption and B) emission spectra ($\lambda_{ex}=350$ nm) of **NDI-NA** (1×10^{-4} M) in various ratios of MCH (0–95%) in $CHCl_3$ at rt. Arrows indicate how the absorption and emission intensities change upon increasing the MCH percentage in $CHCl_3$.

358, 340, and 380 nm, which is typical for a π–π^* transition. The UV/Vis absorption exhibits significant decrease in UV/Vis absorption peak intensity with a loss of the fine structures along with an increase of absorption peak at 404 nm in varying ratios of MCH in chloroform. These results are attributed to the aggregation of the **NDI-NA** in nonpolar solvent. Furthermore, fluorescence spectroscopy was used to investigate the AIEE effect of **NDI-NA** in chloroform/MCH mixes. Figure 3B shows the fluorescence emission spectrum of the compound **NDI-NA** in chloroform and shows rather weak fluorescence emission bands at 408 nm, 430 nm, and 462 nm ($\Phi_F=1.3\%$). However, upon addition of MCH (0–95%), the emission bands at 408 and 430 nm merged, and the emission band at 415 nm, along with bands at 525 nm and 560 nm, emerged and with a gradual increase in intensity (Figure S1 in the Supporting Information). This enhancement in fluorescence with a high quantum yield ($\Phi_F=22.8\%$) observed for **NDI-NA** upon addition of MCH is attributed to the AIEE effect within the aggregates.

Time-dependent density functional theory (TD-DFT) calculations using B3LYP/6-311G level of theory for eight excitations (electronic transitions) of **NDI-NA** in the gas phase was conducted using the Gaussian 09 suite of programs[29] (Figure 4). The results show that HOMO→LUMO optical transition occurs at 469 nm but with very weak oscillator strength $f=0.0012$. The main transition obtained from the ab initio calculation is H-8 and H-2→L at 378 and 373 nm with oscillator strengths of $f=0.1375$ and 0.2725, respectively. This is in agreement with the UV/Vis spectrum of **NDI-NA**. Theoretical study of the **NDI-NA** molecule shows that the HOMO orbital is concentrated on

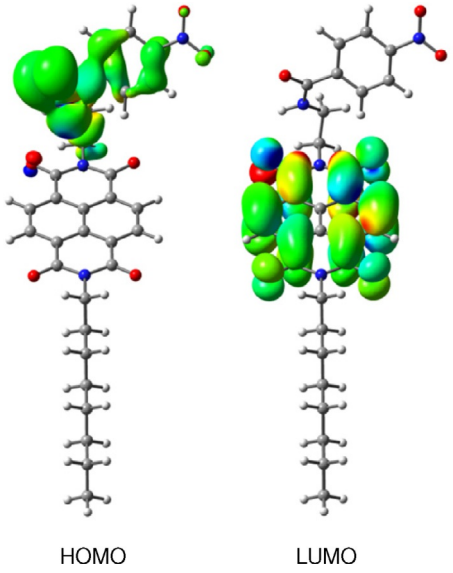

Figure 4. Electron density map of HOMO and LUMO orbitals of **NDI-NA**.

the amide nitro benzene moiety (electron donor), while the LUMO is concentrated on the NDI core (electron acceptor), Figure 3. This transition is not allowed in the unassociated molecule as obtained from theoretical calculations, but this transition becomes dominant when molecule is associated in a self-assembly aggregate via H-bonding and π–π stacking interactions.

The electronic excitation energies and the corresponding oscillator strengths and configuration interaction coefficients of the low-lying excited states of **NDI-NA** are listed in Table S1 in the Supporting Information, and the predicted UV/Vis and circular dichroism (CD) spectra are shown in Figure S6 in the Supporting Information. TD-DFT for **NDI-N** molecules found both the HOMO and the LUMO are located on the nitrobenzene moiety with high oscillator strength ($f=0.4459$) at 374 nm. The electron density on the NDI moiety becomes significant only at the higher exited states of LUMO+1 and LUMO+2. So the HOMO–LUMO transition is not affected by the aggregation of **NDI-N** nor the rigidity of the NDI structure and nitrobenzene moieties (see Figure S2 in the Supporting Information).

We examined the naked-eye AIEE effect of **NDI-N** and **NDI-NA** in a chloroform/MCH solvent system. **NDI-N** exhibits very week blue emission in chloroform, and, upon incremental addition of MCH (0–95%), no change in emission color or intensity was observed (Figure S3 in the Supporting Information).The weak emission of **NDI-N** could be due to the molecular dissolution in the chloroform/MCH mixtures. However, **NDI-NA** is non-emissive in chloroform, whereas it turns on in the visible region upon incremental addition of MCH (0–95%), as shown in Figure 5. These results confirm that **NDI-NA** is AIEE active in aggregated states. These results encouraged us to further investigate the self-assembly of **NDI-NA** using scanning electron microscopy (SEM) and transmission electron microscopy (TEM).

The **NDI-NA** (1.5×10^{-4} M) was dissolved in chloroform/MCH (5:95, *v/v*), and a 20 μL droplet was applied directly to a glass coverslip substrate. After solvent evaporation, the solid was

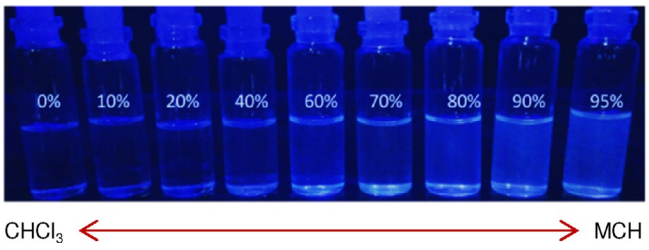

Figure 5. NDI-NA (1×10^{-4} M) in solution in varying concentrations of MCH (0–95 %) in $CHCl_3$ taken under 365 nm hand-lamp irradiation.

sputter-coated with gold for 10 s at 0.016 mA Ar plasma (SPI, West Chester, USA). Self-assembled micro and nanostructures were examined using field-emission (FE)-SEM (FEI Nova Nano-SEM Hillsboro, USA) operating at high vacuum. The SEM technique provided direct visualization of the self-assembled morphology of **NDI-NA** (Figure 6). **NDI-NA** formed multilayer high

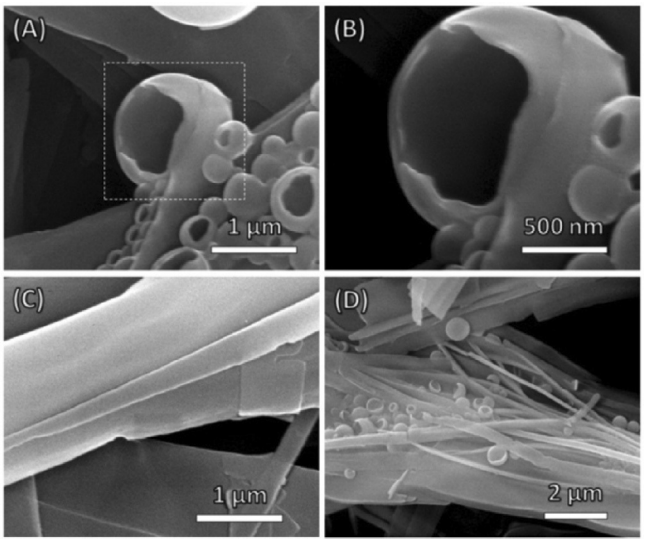

Figure 6. SEM micrograph of A) the **NDI-NA** in the microsheet and nanocapsules in $CHCl_3$/MCH (*v/v*; 5:95), B) an enlarged area where sheets are shown to be bent to form the initial shape of the microcapsule structure, C) multilayered flat sheets with thickness in the range of few nm, and D) microsheets and cup-shaped structures which, in some cases, grew into complete microcapsules.

aspect ratio sheets 10–100 nm in thickness and up to 20 μM in length from chloroform/MCH (*v/v*, 5:95). The sheets coexisted with vesicles at various stages of formation. Incomplete shells initially formed from curved nanosheets to produce a micelle, which could further collapse to decrease surface energy and form microcups. There exists a dynamic equilibrium between the solvated **NDI-NA** molecules and the sharply curved edges of these microcups resulting in its further growth to form a vesicle, this mechanism can continue to result in multilayer vesicles (Figure 6 A,B). The image in Figure 6 C,D shows that the nanosheets, microcups, and microcapsules were all present together. We suggest that the formation of sheets, microcups, and vesicles is a function of the concentration of **NDI-NA** at various stages of solvent evaporation and solid phase separation. At high concentrations the aggregation proceeds to form large high-aspect-ratio sheets and further stacking of these sheets to form multilayered structures. The directional growth of these sheets indicates a preferred orientation in the aggregates directed by the direction of the H-bonding and π–π-stacking of the NDI core. At low concentration of **NDI-NA**, initially single-layer, small, flat aggregates form. These small flat self-assemblies contain high surface and edge free energies. The assembly structure tends to go through bending and fusion to relieve edge free energy and further stabilize the structure to form micelles, cups, and finally, vesicles.

Increasing the MCH ratio in the solvent enhances the solvation of the flat sheet aggregates by interacting with each other, thus forming a large sheet. In the presence of chloroform/MCH (10:90, *v/v*) only nanosheets were observed (see Figure S4 in the Supporting Information). These results clearly indicate that MCH concentration is crucial to the molecular organization and introduces bending and fusion required to form microcups. However, **NDI-N** failed to assemble into any structures in any proportion of chloroform/MCH as shown in Figure S5 in the Supporting Information. This indicates the importance of the amide subunit in molecular self-assembly and its contribution of strong H-bonding in a mixture of hydrophobic solvents.

To gain more structural information, TEM was employed to investigate the **NDI-NA** self-assembled nanostructures in chloroform/MCH (5:95, *v/v*). For TEM analysis, the **NDI-NA** sample was deposited on holey carbon grids by solvent evaporation. Similar to the SEM images, sheets, microcups, and vesicular structures could be found from TEM images of the chloroform/MCH (5:95, *v/v*) sample (Figure 7 and Figure S6 in the Supporting Information). The stages of complete vesicle formation from bowl-like structures are illustrated in Figure 6 D–F. The **NDI-NA** vesicles were, on average, 460 nm in diameter with wall thickness of about 70 nm.

Powder X-ray diffraction (PXRD) of **NDI-NA** has a crystalline nature after self-assembly in chloroform/MCH (5:95, *v/v*); however, it shows noncrystalline solid properties in nature (Figure S7 in the Supporting Information).

The dynamic light scattering (DLS) measurements in chloroform/MCH (5:95, *v/v*) further confirmed the vesicular aggregates. Size distribution in DLS showed vesicular aggregates with an average diameter of 512 nm (Figure S5 in the Supporting Information). The smaller vesicular size determined by TEM as compared with DLS is most likely due to the drying effect on the surface. Fluorescence (FL) spectra ($\lambda_{ex}=350$ nm) of **NDI-NA** (1×10^{-4} M) in chloroform, chloroform/MCH (5:95, *v/v*), and the solid state at room temperature (Figure S9 in the Supporting Information) show that the solid noncrystalline material has a similar weak fluorescence like NDI-NA in its dissolved state in chloroform.

To gain further insight into the hydrogen bonding in the self-assembled nanostructures, we examined the IR spectra of the **NDI-NA** in solid, solution, and self-assembled states (Figure 8). The FT-IR spectrum of **NDI-NA** in the solid state and as well-solvated molecules in chloroform (where there is less

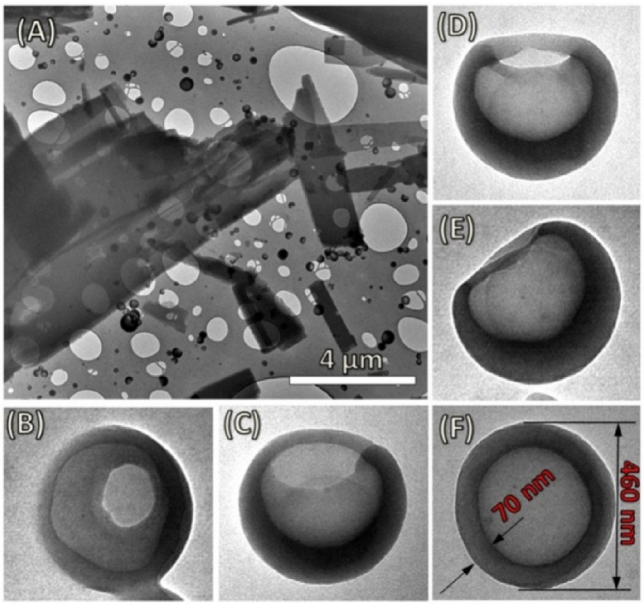

Figure 7. TEM images of the **NDI-NA** in aggregation state in organic solvents such as $CHCl_3$/MCH (*v/v*; 5:95).

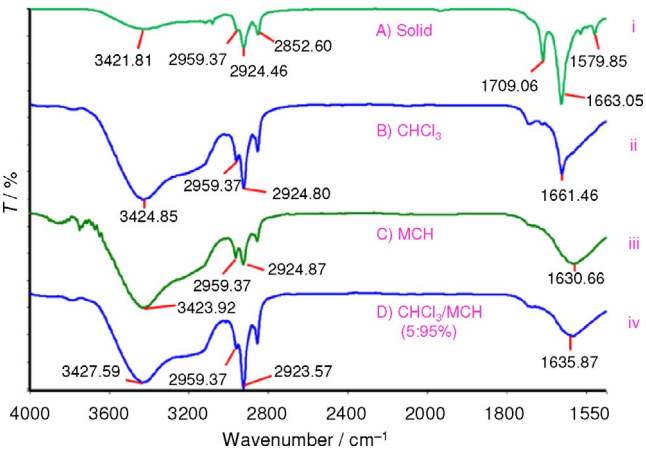

Figure 8. FT-IR spectra of **NDI-NA** in i) solid state, ii) $CHCl_3$, iii) MCH, and iv) $CHCl_3$/MCH (5:95%, *v/v*).

chance of aggregation and H-bonding) exhibit two typical peaks at 1663 cm^{-1} and 1579 cm^{-1}. These were ascribed to amide-I and amide-II, which are primarily due to the stretching vibration of amide carbonyl and the N–H out-of-plane bending mode, respectively. However, the self-assembled state of **NDI-NA** in chloroform/MCH (5:95, *v/v*) and in only MCH showed obvious changes in the amide peak shape and positions; the amide-I band was broadened and appeared at 1635 and 1630 cm^{-1}, respectively, while the amide-II band was attenuated. This clearly indicates that the amide hydrogen bonding was one of the main driving forces for **NDI-NA** self-assembly.

Conclusion

The parameters in **NDI-NA** molecular design intended to introduce electron donor (nitrophenyl) and electron acceptor (NDI core) moieties in the structure spaced by an imide group to decrease the HOMO–LUMO transition in the well-solvated molecule. This molecular engineering also considered the self-association interactions to induce supramolecular micro and nano structures via amide H-bonding, π–π stacking of the NDI cores, and hydrophobic interactions between the alkyl moieties, which can be balanced using solvophobic control. The self-assembly process has resulted in aggregation-induced emission enhancement (AIEE) due to restricted intramolecular rotation. The self-assembly process was influenced by chemical interactions and thermodynamic surface and edge free energies and solvation energies. At higher concentrations and upon solvent evaporation, aggregates tend to grow in 2D, resulting in phase separation in the form of single and multilayered sheets in chloroform/MCH (5:95%, *v/v*). The reduction of **NDI-NA** after this stage results in the formation of small single-layer sheets which further bend and fuse to form micelles. Large unstable micelles collapsed to form microcups about 0.5 μm in diameter. The microcups in equilibrium with solvated **NDI-NA** further grew to form fully formed vesicles (see Figure 1). In the absence of amide functionality within the structure, i.e. **NDI-N**, no assembly was observed, indicating the fundamental role of H-bonding in the self-association process. The present study paves the way for the rational and controlled designs of nanostructures made of AIEE-active dyes, which may open a new avenue towards tuning well-controlled fluorescence architectures.

Experimental Section

General methods and materials

Reagents were received from Sigma Aldrich Chemical Co. (Bangalore, Karnataka, India) and used without further purification. Solvents were purchased from commercial sources from Hyderabad, Telangana, India-based companies and purified by reported protocols. Spectroscopic-grade solvents were used for physical studies. ^1H and ^{13}C NMR spectra were recorded on Bruker −300 MHz and 500 MHz machines and calibrated against tetramethylsilane (TMS). UV/Vis absorption experiments were performed on a UV-1800 Shimadzu spectrophotometer. Photoluminescence studies were performed in a Cary Eclipse fluorescence spectrophotometer. Mass spectrometric data were acquired by an electrospray ionization (ESI) technique on a Q-TOF-micro quadruple mass spectrometer.

UV/Vis absorption spectroscopy

The stock solutions (1×10^{-3} M) of **NDI-N** and **NDI-NA** were prepared in $CHCl_3$. An aliquot of it was transferred to various ratios of $CHCl_3$/MCH in different volumetric flasks (final volume of 2 mL) and allowed to equilibrate for 2 h prior to the UV/Vis absorption measurements.

Fluorescence spectroscopy

Fluorescence emission spectra were measured in a Fluoromax-4 spectrofluorometer. All experiments were performed upon excitation at 350 nm in a quartz cell with a 1 cm path length. The stock

solutions were prepared in a similar manner as for the absorption study and employed for emission measurements.

Sample preparation

The stock solutions were prepared in $CHCl_3$ in a similar manner as for the UV/Vis study. The solutions were allowed to equilibrate for 2 h at rt.

Scanning electron microscopy

SEM images of **NDI-N** and **NDI-NA** were recorded on an FEI Nova NanoSEM (Hillsboro, OR USA) operating at high vacuum. For SEM imaging, the samples of **NDI-A** and **NDI-NA** were sputter-coated with gold for 10 s at 0.016 mA Ar plasma after drop-casting the solutions on glass coverslip and solvent evaporation at rt.

Transmission electron microscopy

TEM samples were prepared by the paper blotting method followed by solvent evaporation on a holey carbon-coated copper grid. The micrographs were measured using a JEOL 1010 100 kV transmission electron microscope.

Infrared spectroscopy

FT-IR spectra were recorded on a PerkinElmer Spectrum spectrometer. The liquid sample in $CHCl_3$/MCH (5:95, *v/v*) was drop-casted and solvent was allowed to evaporate on the surface naturally.

Acknowledgements

S. V. B. (RMIT) acknowledges financial support from the Australian Research Council under a Future Fellowship Scheme (FT110100152) and the RMIT Microscopy and Microanalysis Facility (RMMF). S. V. B. (IICT) is grateful for financial support from the Department of Atomic Energy–Board of Research in Nuclear Sciences (DAE-BRNS), Mumbai (Project Code 37(2)/14/08/2014-BRNS) and Intelcoat, CSIR, New Delhi, India (Project CSC0114). N. V. G. acknowledges CSIR, New Delhi, for Senior Research Fellowship (SRF) support. R. S. B acknowledges financial support from CSIR, New Delhi under the Senior Research Associateship (SRA) Scheme 13(8772)-A)/2015-Pool.

Keywords: aggregation-induced emission · amphiphile · cup-like morphology · nanostructures · naphthalene diimides · self-assembly

[1] a) Anuradha, D. D. La, M. Al Kobaisi, S. V. Bhosale, *Sci. Rep.* **2015**, *5*, 15652; b) R. S. Bhosale, M. Al Kobaisi, S. V. Bhosale, S. Bhargava, S. V. Bhosale, *Sci. Rep.* **2015**, *5*, 14609 c) S. V. Bhosale, S. V. Bhosale, *Sci. Rep.* **2013**, *3*, 1982; d) S. V. Bhosale, *Chem. Eur. J.* **2014**, *20*, 5253.

[2] a) S. V. Bhosale, S. V. Bhosale, S. R. Bobe, G. V. Shitre, A. Gupta, *Eur. J. Org. Chem.* **2013**, 3939; b) S. V. Bhosale, M. Adsul, G. V. Shitre, S. R. Bobe, S. V. Bhosale, S. Privér, *Chem. Eur. J.* **2013**, *19*, 7310; c) A. Rananaware, D. D. La, S. V. Bhosale, *RSC Adv.* **2015**, *5*, 56270; d) A. Rananaware, R. S. Bhosale, K. Ohkubo, H. Patil, L. S. Jones, S. Fukuzumi, S. V. Bhosale, S. V. Bhosale, *J. Org. Chem.* **2015**, *80*, 3832.

[3] a) J. Chen, F. Cheng, *Acc. Chem. Res.* **2009**, *42*, 713; b) S. I. Stupp, *Nano Lett.* **2010**, *10*, 4783; c) J. M. Warman, M. P. De Haas, G. Dicker, F. C. Grozema, J. Piris, M. G. Debije, *Chem. Mater.* **2004**, *16*, 4600; d) L. Cademartiri, G. A. Ozin, *Adv. Mater.* **2009**, *21*, 1013; e) J. M. Warman, A. M. Ven de Craata, *Mol. Cryst. Liq. Cryst.* **2003**, *396*, 41.

[4] a) M. R. Molla, S. Ghosh, *Chem. Mater.* **2011**, *23*, 95; b) M. R. Molla, S. Ghosh, *Chem. Eur. J.* **2012**, *18*, 1290; c) A. Das, S. Ghosh, *Angew. Chem. Int. Ed.* **2014**, *53*, 1092; *Angew. Chem.* **2014**, *126*, 1110; d) O. Ivasenko, D. F. Perepichka, *Chem. Soc. Rev.* **2011**, *40*, 191; e) D. González-Rodríguez, A. P. H. J. Schenning, *Chem. Mater.* **2011**, *23*, 310; f) G. D. Pantoş, P. Pengo, J. K. M. Sanders, *Angew. Chem.* **2007**, *119*, 198; *Angew. Chem. Int. Ed.* **2007**, *46*, 194; *Angew. Chem.* **2007**, *119*, 198; g) O. Yushchenko, R. V. Hangarge, S. Mosquera-Vazquez, S. V. Bhosale, E. Vauthey, *J. Phys. Chem. B* **2015**, *119*, 7308–7320; h) D. Villamaina, M. M. A. Kelson, S. V. Bhosale, E. Vauthey, *Phys. Chem. Chem. Phys.* **2014**, *16*, 5188.

[5] a) S. V. Bhosale, C. H. Jani, S. J. Langford, *Chem. Soc. Rev.* **2008**, *37*, 331; b) N. Sakai, J. Mareda, E. Vauthey, S. Matile, *Chem. Commun.* **2010**, *46*, 4225–4237; c) S. V. Bhosale, S. V. Bhosale, S. K. Bhargava, *Org. Biomol. Chem.* **2012**, *10*, 6455.

[6] a) S. Guha, S. Saha, *J. Am. Chem. Soc.* **2010**, *132*, 17674; b) M. Ajayakumar, S. Yadav, S. Ghosh, P. Mukhopadhyay, *Org. Lett.* **2010**, *12*, 2646; c) N. V. Ghule, R. S. Bhosale, K. Kharat, A. L. Puyad, S. V. Bhosale, S. V. Bhosale, *ChemPlusChem* **2015**, *80*, 485; d) C. Zhou, Y. Li, Y. Zhao, J. Zhang, W. Yang, Y. Li, *Org. Lett.* **2011**, *13*, 292; e) S. V. Bhosale, S. V. Bhosale, M. B. Kalyankar, S. J. Langford, *Org. Lett.* **2009**, *11*, 5418.

[7] a) B. J. H. Oh, S. L. Suraru, W. Y. Lee, M. Könemann, H. W. Höffken, C. Röger, R. Schmidt, Y. Chung, W. C. Chen, F. Würthner, Z. Bao, *Adv. Funct. Mater.* **2010**, *20*, 2148; b) B. A. Jones, A. Facchetti, M. R. Wasielewski, T. J. Marks, *J. Am. Chem. Soc.* **2007**, *129*, 15259; c) H. E. Katz, A. J. Lovinger, J. Johnson, C. Kloc, T. Siegrist, W. Li., Y. Y. Lin, A. Dodabalapur, *Nature* **2000**, *404*, 478.

[8] a) H. Patil, A. Gupta, A. Bilic, S. V. Bhosale, S. V. Bhosale, *Tetrahedron Lett.* **2014**, *55*, 4430; b) S. R. Bobe, A. Gupta, A. Rananaware, A. Bilic, S. V. Bhosale, S. V. Bhosale, *RSC Adv.* **2015**, *5*, 4411.

[9] a) S. Bhosale, A. L. Sisson, P. Talukdar, A. Fürstenberg, N. Banerji, E. Vauthey, G. Bollot, J. Mareda, C. Röger, F. Würthner, N. Sakai, S. Matile, *Science* **2006**, *313*, 84; b) M. M. A. Kelson, R. S. Bhosale, K. Ohkubo, L. A. Jones, S. V. Bhosale, A. Gupta, S. Fukuzumi, S. V. Bhosale, *Dyes Pigm.* **2015**, *120*, 340–346.

[10] a) A. Milelli, V. Tumiatti, M. Micco, M. Rosini, G. Zuccari, L. Raffaghello, G. Bianchi, V. Pistoia, J. Fernando Díaz, B. Pera, C. Trigili, I. Barasoain, C. Musetti, M. Toniolo, C. Sissi, S. Alcaro, F. Moraca, M. Zini, C. Stefanelli, A. Minarini, *Eur. J. Med. Chem.* **2012**, *57*, 417; b) G. A. Parkinson, F. Cuenca, N. J. Stephen, *Mol. Biol.* **2008**, *381*, 1145; c) M. Gunaratnam, M. dlFuente, S. M. Hampel, A. K. Todd, A. P. Reszka, A. Schätzlein, S. Neidle, *Bioorg. Med. Chem.* **2011**, *19*, 7151.

[11] K. P. Nandre, S. V. Bhosale, K. V. S. Rama Krishna, A. Gupta, S. V. Bhosale, *Chem. Commun.* **2013**, *49*, 5444.

[12] H. Shao, M. Gao, S. H. Kim, C. P. Jaroniec, J. R. Parquette, *Chem. Eur. J.* **2011**, *17*, 12882.

[13] S. Hagihara, L. Gremaud, G. Bollot, J. Mareda, S. Matile, *J. Am. Chem. Soc.* **2008**, *130*, 4347.

[14] H. Shao, J. R. Paraquette, *Chem. Commun.* **2010**, *46*, 4285.

[15] P. Mukhopadhyay, Y. Iwashita, M. Shirakawa, S.-i. Kawano, N. Fujita, S. Shinkai, *Angew. Chem. Int. Ed.* **2006**, *45*, 1592; *Angew. Chem.* **2006**, *118*, 1622.

[16] a) H. Y. Au-Yeung, G. D. Pantos, J. K. M. Sanders, *Proc. Natl. Acad. Sci. USA* **2009**, *106*, 10466; b) H. Y. Au-Yeung, G. D. Pantos, J. K. M. Sanders, *Angew. Chem. Int. Ed.* **2010**, *49*, 5331; *Angew. Chem.* **2010**, *122*, 5459.

[17] T. Iijima, S. A. Vignon, H. R. Tseng, T. Jarrosson, J. K. M. Sandres, F. Marchioni, M. Venturi, E. Apostoli, E. Balazni, J. F. Stoddart, *Chem. Eur. J.* **2004**, *10*, 6375.

[18] a) R. Scott Lokey, B. L. Iverson, *Nature* **1995**, *375*, 303; b) J. J. Reczek, K. R. Villazor, V. Lynch, T. M. Swager, B. L. Iverson, *J. Am. Chem. Soc.* **2006**, *128*, 7995; c) S. De, S. Ramakrishnan, *Chem. Asian J.* **2011**, *6*, 149.

[19] M. Kumar, S. J. George, *Nanoscale* **2011**, *3*, 2130.

[20] L. E. Euliss, J. A. DuPont, S. Gratton, J. DeSimone, *Chem. Soc. Rev.* **2006**, *35*, 1095.

[21] a) K. P. Nandre, M. A. Kobaisi, R. S. Bhosale, K. Latham, S. V. Bhosale, S. V. Bhosale, *RSC Adv.* **2014**, *4*, 40381; b) S. Datta, S. Bhattacharya, *Chem. Commun.* **2012**, *48*, 877; c) M.-O. M. Piepenbrock, N. Clarke, J. A. Foster, J. W. Steed, *Chem. Commun.* **2011**, *47*, 2095; d) J. R. Moffat, D. K. Smith, *Chem. Commun.* **2011**, *47*, 11864.

[22] a) Y. N. Hong, J. W. Y. Lam, B. Z. Tang, *Chem. Soc. Rev.* **2011**, *40*, 5361; b) Z. G. Chi, X. Q. Zhang, B. J. Xu, X. Zhou, C. P. Ma, Y. Zhang, S. W. Liu, J. R. Xu, *Chem. Soc. Rev.* **2012**, *41*, 3878.

[23] a) R. Misra, T. Jadhav, B. Dhokale, S. M. Mobin, *Chem. Commun.* **2014**, *50*, 9076; b) Y. You, H. S. Huh, K. S. Kim, S. W. Lee, D. Kim, S. Y. Park, *Chem. Commun.* **2008**, 3998.

[24] a) B. K. An, S. K. Kwon, S. D. Jung, S. Y. Park, *J. Am. Chem. Soc.* **2002**, *124*, 14410; b) Y. Qian, S. Li, G. Zhang, Q. Wang, S. Wang, H. Xu, C. Li, Y. Li, G. Q. Yang, *J. Phys. Chem. B* **2007**, *111*, 5861.

[25] a) F. K.-W. Hau, T. K.-M. Lee, E. C.-C. Cheng, V. K.-M. Au, V. W.-W. Yam, *Proc. Natl. Acad. Sci. USA* **2014**, *111*, 15900; b) W. X. Ni, M. Li, J. Zheng, S. Z. Zhan, Y. M. Qiu, S. W. Ng, D. Li, *Angew. Chem. Int. Ed.* **2013**, *52*, 13472; *Angew. Chem.* **2013**, *125*, 13714; c) Z. Luo, X. Yuan, Y. Yu, Q. Zhang, D. T. Leong, J. Y. Lee, J. Xie, *J. Am. Chem. Soc.* **2012**, *134*, 16662.

[26] a) Q. Zhao, L. Li, F. Li, M. Yu, Z. Liu, T. Yi, C. Huang, *Chem. Commun.* **2008**, 685; b) K. Huang, H. Wu, M. Shi, F. Li, T. Yi, C. Huang, *Chem. Commun.* **2009**, 1243.

[27] a) D. Yan, *Chem. Eur. J.* **2015**, *21*, 4880; b) D. Yan, D.-K. Bučar, A. Delori, B. Patel, G. O. Lloyd, W. Jones, X. Duan, *Chem. Eur. J.* **2013**, *19*, 8213; c) D. Yan, W. Jones, G. Fan, M. Wei, D. G. Evans, *J. Mater. Chem. C* **2013**, *1*, 4138; d) D. Yan, Y. Lin, Q. Meng, M. Zhao, M. Wei, *Cryst. Growth Des.* **2013**, *13*, 4495; e) D. Yan, G. R. Williams, M. Zhao, C. Li, G. Fan, H. Yang, *Langmuir* **2013**, *29*, 15673.

[28] a) Y. Zhang, J.-H. Wang, J. Zheng, D. Li, *Chem. Commun.* **2015**, *51*, 6350; b) L. Zhu, X. Li, Q. Zhang, X. Ma, M. Li, H. Zhang, Z. Luo, H. Ågren, Y. Zhao, *J. Am. Chem. Soc.* **2013**, *135*, 5175.

[29] A. Rananaware, D. D. La, S. V. Bhosale, *RSC Adv.* **2015**, *5*, 63130.

[30] M. J. Frisch, G. W. Trucks, H. B. Schlegel, G. E. Scuseria, M. A. Robb, J. R. Cheeseman, G. Scalmani, V. Barone, B. Mennucci, G. A. Petersson, H. Nakatsuji, M. Caricato, X. Li, H. P. Hratchian, A. F. Izmaylov, J. Bloino, G. Zheng, J. L. Sonnenberg, M. Hada, M. Ehara, K. Toyota, R. Fukuda, J. Hasegawa, M. Ishida, T. Nakajima, Y. Honda, O. Kitao, H. Nakai, T. Vreven, J. A. Montgomery Jr., J. E. Peralta, F. Ogliaro, M. Bearpark, J. J. Heyd, E. Brothers, K. N. Kudin, V. N. Staroverov, T. Keith, R. Kobayashi, J. Normand, K. Ragahavachari, A. Rendell, J. C. Burant, S S. Iyengar, J. Tomasi, M. Cossi, N. Rega, J. M. Millam, M. Klene, J. E. Knox, J. B. Cross, V. Bakken, C. Adamo, J. Jaramillo, R. Gomperts, R. E. Stratmann, O. Yazyev, A. J. Austin, R. Cammi, C. Pomelli, J. W. Ochterski, R. L. Martin, K. Morokuma, V. G. Zakrzewski, G. A. Voth, P. Salvador, J. J. Dannenberg, S. Dapprich, A. D. Daniels, O. Farkas, J. B. Foresman, J. V. Ortiz, J. Cioslowski, D. J. Fox, Gaussian 09, Revision D.01, Gaussian, Inc., Wallingford CT, **2013**.

Received: October 27, 2015
Published online on January 11, 2016

